

6-14-2012

Hyperbolic metamaterial interfaces: Hawking radiation from Rindler horizons and spacetime signature transitions

Igor I. Smolyaninov
University of Maryland College Park

Ehren R. Hwang
University of Maryland College Park

Evgenii Narimanov
Birck Nanotechnology Center, Purdue University, evgenii@purdue.edu

Follow this and additional works at: <http://docs.lib.purdue.edu/nanopub>

Smolyaninov, Igor I.; Hwang, Ehren R.; and Narimanov, Evgenii, "Hyperbolic metamaterial interfaces: Hawking radiation from Rindler horizons and spacetime signature transitions" (2012). *Birck and NCN Publications*. Paper 1177.
<http://dx.doi.org/10.1103/PhysRevB.85.235122>

This document has been made available through Purdue e-Pubs, a service of the Purdue University Libraries. Please contact epubs@purdue.edu for additional information.

Hyperbolic metamaterial interfaces: Hawking radiation from Rindler horizons and spacetime signature transitions

Igor I. Smolyaninov,^{1,*} Ehren Hwang,¹ and Evgenii Narimanov²

¹*Department of Electrical and Computer Engineering, University of Maryland, College Park, Maryland 20742, USA*

²*Birck Nanotechnology Centre, School of Electrical and Computer Engineering, Purdue University, West Lafayette, Indiana 47907, USA*

(Received 19 March 2012; published 14 June 2012)

Extraordinary rays in a hyperbolic metamaterial behave as particle world lines in a three-dimensional (2 + 1) Minkowski spacetime. We analyze electromagnetic field behavior at the boundaries of this effective spacetime depending on the boundary orientation. If the boundary is perpendicular to the spacelike direction in the metamaterial, an effective Rindler horizon may be observed, which produces Hawking radiation. On the other hand, if the boundary is perpendicular to the timelike direction, the system undergoes a phase transition to a state with a different nature of the spacetime, with nonintegrable field divergence at the transformation point. Experimental observations of the transition using plasmonic metamaterials confirm this conclusion.

DOI: [10.1103/PhysRevB.85.235122](https://doi.org/10.1103/PhysRevB.85.235122)

PACS number(s): 78.20.Ci

Modern developments in gravitation research strongly indicate that classic general relativity is an effective macroscopic field theory, which needs to be replaced with a more fundamental theory based on yet unknown microscopic degrees of freedom. On the other hand, our ability to obtain experimental insights into the future fundamental theory is strongly limited by low energy scales available to terrestrial particle physics and astronomical observations. The emergent analog spacetime program offers a promising way around this difficulty. Looking at such systems as superfluid helium and cold atomic Bose-Einstein condensates, physicists learn from nature and discover how macroscopic field theories arise from known well-studied atomic degrees of freedom. An interesting recent example of this approach is Horava gravity,¹ which is based on the well-known Lifshitz point behavior in solid state physics. Another exciting development along this direction is the recent introduction of metamaterials and transformation optics.²⁻⁴ The latter field is not limited by the properties of atoms and molecules given to us by nature. “Artificial atoms” used as building blocks in metamaterial design offer much more freedom in constructing analogs of various exotic spacetime metrics, such as black holes,⁵⁻⁹ wormholes,^{10,11} spinning cosmic strings,¹² and even the metric of Big Bang itself.¹³ Explosive development of this field promises new insights into the fabric of spacetime, which cannot be gleaned from any other terrestrial experiments.

On the other hand, compared to standard general relativity, metamaterial optics gives more freedom to design an effective spacetime with very unusual properties. Light propagation in all static general relativity situations can be mimicked with positive $\varepsilon_{ik} = \mu_{ik}$,¹⁴ while the allowed parameter space of the metamaterial optics is broader. Thus, flat Minkowski spacetime with the usual $(-, +, +, +)$ signature does not need to be a starting point. Other effective signatures, such as the “two times” (2T) physics $(-, -, +, +)$ signature may be realized.¹⁵ Theoretical investigation of the 2T higher dimensional spacetime models had been pioneered by Dirac.¹⁶ More recent examples can be found in Refs. 17 and 18. Metric signature change events (in which a phase transition occurs between say $(-, +, +, +)$ and $(-, -, +, +)$ spacetime signature) are being studied in Bose-Einstein condensates

and in some modified gravitation theories (see Ref. 19 and the references therein). It is predicted that a quantum field theory residing on a spacetime undergoing a signature change reacts violently to the imposition of the signature change. Both the total number and the total energy of the particles generated in a signature change event are formally infinite.¹⁹ While optics of bulk hyperbolic metamaterials provide us with ample opportunities to observe metric signature transitions,¹⁵ even more interesting physics arise at the metamaterial interfaces. Very recently it was demonstrated that mapping of monochromatic extraordinary light distribution in a hyperbolic metamaterial along some spatial direction may model the “flow of time” in a three-dimensional (3D) (2 + 1) effective Minkowski spacetime.¹³ If an interface between two metamaterials is engineered so that the effective metric changes signature across the interface, two possibilities may arise. If the interface is perpendicular to the timelike direction z , this coordinate does not behave as a “timelike” variable any more, and the continuous “flow of time” is interrupted. This situation (which cannot be realized in classic general relativity) may be called the “end of time.” It appears that optics of metamaterials near the “end of time” event is quite interesting and deserves a detailed study. For example, in the lossless approximation all the possible “end of time” scenarios lead to field divergencies, which indicate quite interesting linear and nonlinear optics behavior near the “end of time.” On the other hand, if the metamaterial interface is perpendicular to the spacelike direction of the effective (2 + 1) Minkowski spacetime, a Rindler horizon may be observed (the Rindler metric approximates spacetime behavior near the black hole event horizon).¹⁴

Let us begin with a brief summary of Refs. 13 and 15, which demonstrated that a spatial coordinate may become “timelike” in a hyperbolic metamaterial. To better understand this effect, let us start with a nonmagnetic uniaxial anisotropic material with dielectric permittivities $\varepsilon_x = \varepsilon_y = \varepsilon_1$ and $\varepsilon_z = \varepsilon_2$ and assume that this behavior holds in some frequency range around $\omega = \omega_0$. Any electromagnetic field propagating in this material can be expressed as a sum of the “ordinary” and “extraordinary” contributions, each of these being a sum of an arbitrary number of plane waves polarized in the “ordinary”

(\vec{E} perpendicular to the optical axis) and “extraordinary” (\vec{E} parallel to the plane defined by the k vector of the wave and the optical axis) directions. Let us define our “scalar” extraordinary wave function as $\varphi = E_z$ so that the ordinary portion of the electromagnetic field does not contribute to φ . Since metamaterials exhibit high dispersion, let us work in the frequency domain and write the macroscopic Maxwell equations as²⁰

$$\frac{\omega^2}{c^2} \vec{D}_\omega = \vec{\nabla} \times \vec{\nabla} \times \vec{E}_\omega \quad \text{and} \quad \vec{D}_\omega = \vec{\varepsilon}_\omega \vec{E}_\omega. \quad (1)$$

Equation (1) results in the following wave equation for φ_ω if ε_1 and ε_2 are kept constant inside the metamaterial:

$$-\frac{\omega^2}{c^2} \varphi_\omega = \frac{\partial^2 \varphi_\omega}{\varepsilon_1 \partial z^2} + \frac{1}{\varepsilon_2} \left(\frac{\partial^2 \varphi_\omega}{\partial x^2} + \frac{\partial^2 \varphi_\omega}{\partial y^2} \right). \quad (2)$$

While in ordinary crystalline anisotropic media both ε_1 and ε_2 are positive, this is not necessarily the case in metamaterials. In hyperbolic metamaterials²¹ ε_1 and ε_2 have opposite signs. These metamaterials are typically composed of multilayer metal-dielectric or metal wire array structures, as shown in Fig. 1. Optical properties of such metamaterials are quite extraordinary. For example, there is no usual diffraction limit in a hyperbolic metamaterial.^{22,23}

Let us consider the case of constant $\varepsilon_1 > 0$ and $\varepsilon_2 < 0$ and assume that this behavior holds in some frequency range around $\omega = \omega_0$. Let us assume that the metamaterial is illuminated by coherent continuous wave (CW) laser field at frequency ω_0 , and we study spatial distribution of the extraordinary field φ_ω at this frequency. Under these assumptions Eq. (2) can be rewritten in the form of 3D Klein–Gordon equation describing a massive scalar φ_ω field:

$$-\frac{\partial^2 \varphi_\omega}{\varepsilon_1 \partial z^2} + \frac{1}{|\varepsilon_2|} \left(\frac{\partial^2 \varphi_\omega}{\partial x^2} + \frac{\partial^2 \varphi_\omega}{\partial y^2} \right) = \frac{\omega_0^2}{c^2} \varphi_\omega = \frac{m^{*2} c^2}{\hbar^2} \varphi_\omega, \quad (3)$$

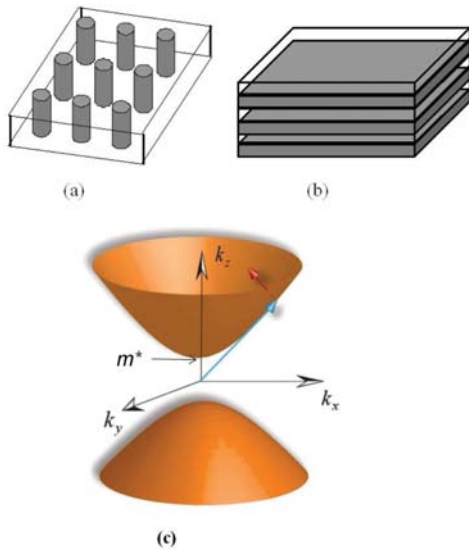


FIG. 1. (Color online) The schematic of the (a) nanowire and (b) layered realizations of hyperbolic media and the (c) corresponding isofrequency surface.

in which the spatial coordinate $z = \tau$ behaves as a “timelike” variable. Therefore, Eq. (3) describes world lines of massive particles, which propagate in a flat $(2+1)$ Minkowski spacetime. When a metamaterial is built and illuminated with a coherent extraordinary CW laser beam, the stationary pattern of light propagation inside the metamaterial represents a complete “history” of a toy $(2+1)$ dimensional spacetime populated with particles of mass m^* . This “history” is written as a collection of particle world lines along the “timelike” z coordinate. Note that in the opposite situation in which $\varepsilon_1 < 0$ and $\varepsilon_2 > 0$, Eq. (2) would describe world lines of tachyons²⁴ having “imaginary” mass $m^* = i\mu$.

The world lines of particles described by Eq. (3) are straight lines, which is easy to observe in the experiment.¹³ If adiabatic variations of ε_1 and ε_2 are allowed inside the metamaterial, world lines of massive particles in some well-known curvilinear spacetimes can be emulated, including the world line behavior near the “beginning of time” at the moment of Big Bang.¹³ Thus, mapping of monochromatic extraordinary light distribution in a hyperbolic metamaterial along some spatial direction may model the “flow of time” in an effective 3D $(2+1)$ spacetime. Since the parameter space of metamaterial optics is broader than the parameter space of general relativity, we can also engineer the “end of time” event if an interface between two metamaterials is prepared so that the effective metric changes signature at the interface. In such a case the spatial coordinate does not behave as a “timelike” variable any more, and the continuous “flow of time” is suddenly interrupted, as shown in Fig. 2(a). While this situation cannot be realized in classic general relativity, the optics of metamaterials near this transition event is quite interesting and deserves a detailed study.

We consider the case of constant $\varepsilon_1 = \varepsilon_x = \varepsilon_y$ and assume that the z -dependent dielectric permittivity component $\varepsilon_2 = \varepsilon_z$ changes sign at $z = 0$. Aside from the relative mathematical simplicity of the model that ignores the spatial variation of the “in-plane” component ε_1 of the dielectric tensor, it also corresponds to the most readily available low-loss realization of hyperbolic metamaterials²⁵ formed by metallic nanowires in dielectric membranes, where in the limit of small volume fraction ($p \ll 1$) and high magnitude of the dielectric permittivity of the metal component with respect to its dielectric counterpart ($-\varepsilon_m \gg \varepsilon_d \sim 1$) the dielectric tensor of the composite equals

$$\varepsilon_x = \varepsilon_y \approx \varepsilon_d \quad (4)$$

$$\varepsilon_z \approx \varepsilon_d + p(z)\varepsilon_m. \quad (5)$$

Taking into account the translational symmetry of the system in x and y directions, we can introduce the in-plane wave vector (k_x, k_y) so that the propagating waves can be expressed as

$$\begin{aligned} E_\omega(\vec{r}) &= E(z) \exp(ik_x x + ik_y y) \\ D_\omega(\vec{r}) &= D(z) \exp(ik_x x + ik_y y) \\ B_\omega(\vec{r}) &= B(z) \exp(ik_x x + ik_y y), \end{aligned} \quad (6)$$

while the uniaxial symmetry of this medium reduces the ordinary and extraordinary waves to, respectively, the TE- ($\vec{E} \perp \hat{z}$) and TM- ($\vec{B} \perp \hat{z}$) polarized modes. Introducing the wavefunction $\psi(\vec{r})$ as the z component of the electric displacement field

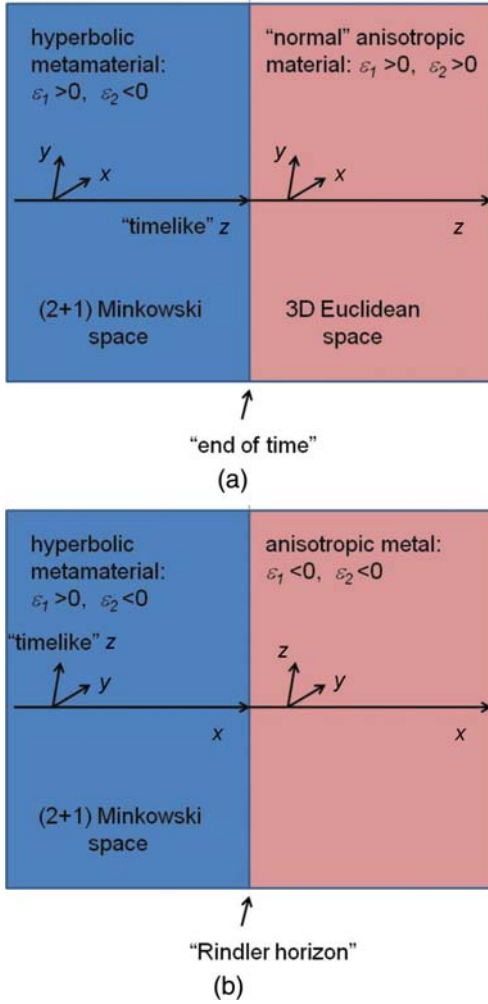


FIG. 2. (Color online) (a) Schematic representation of the “end of time” model in metamaterials: the spatial coordinate z does not behave as a “timelike” variable any more, and the continuous “flow of time” is suddenly interrupted at the interface of two metamaterials. (b) Metric signature change across a “spacelike” direction leads to appearance of a Rindler horizon.

of the TM wave, also proportional to the magnetic field $B(z)$,

$$\psi(\vec{r}) = D_z(\vec{r}) = \varepsilon_z(z)E_z(\vec{r}) = -\frac{c}{\omega}k_x B. \quad (7)$$

For the wave equation we obtain

$$-\frac{\partial^2 \psi}{\partial z^2} + \frac{\varepsilon_1}{\varepsilon_2(z)}\psi = \varepsilon_1 \frac{\omega^2}{c^2}\psi. \quad (8)$$

We will further assume that the material losses in the system are small, so that the propagation distance (and correspondingly the “lifetime” in the proposed model “Universe”) $l \sim (\text{Im}(\varepsilon)/\text{Re}(\varepsilon))\lambda$ is much larger than the thickness d of the area where the dielectric permittivity changes sign:

$$\begin{aligned} \varepsilon_2(z) &= \varepsilon_- + i\Gamma, & \text{at } z \ll -d \\ \varepsilon_2(z) &= \varepsilon_+ = \varepsilon_1, & \text{at } z \gg d. \end{aligned} \quad (9)$$

To avoid the mathematical complications related to nonanalytic behavior of $\varepsilon_2(z)$ but still have a well-defined

transition region near $z = 0$, we assume that the dielectric permittivity exponentially approaches its asymptotic values:

$$\varepsilon_2(z) = \varepsilon_+ \varepsilon_- \frac{1 - \exp(z/d)}{\varepsilon_+ - \varepsilon_- \exp(z/d)} + \frac{i\Gamma}{1 + \left(-\frac{\varepsilon_-}{\varepsilon_+}\right) \exp(z/d)}. \quad (10)$$

Substituting Eq. (10) into Eq. (8), in the limit $\Gamma \ll 1$ we obtain

$$(u^2 + u) \frac{\partial^2 \psi}{\partial u^2} - \frac{Au + B}{u - 1 + i0} \psi = 0, \quad (11)$$

where $u = \exp(z/d)$, and

$$A = (kd)^2 - \varepsilon_1 \left(\frac{\omega d}{c}\right)^2 \quad (12)$$

$$B = \varepsilon_1 \left(\frac{\omega d}{c}\right)^2 - \frac{\varepsilon_1}{\varepsilon_-} (kd)^2. \quad (13)$$

Note that the parameter B is always positive, while $A < 0$ if the dielectric at $z \gg d$ can support the propagating wave with the wave number k (i.e., $k < \sqrt{\varepsilon_+} \omega/c = \sqrt{\varepsilon_1} \omega/c$), and $A > 0$ otherwise. In the former case, a fraction of the energy incident from the hyperbolic medium is transferred to the wave propagating in the dielectric away from the interface, while in the latter the field exponentially decays for $z > 0$.

The general solution of Eq. (11) can be expressed in terms of the hypergeometric function ${}_2F_1(a, b, c, u)$;²⁶ however, care must be taken to choose the proper branch of its analytical continuation as $z = 1$ is a branch point. Physically, the difference between two branches in question corresponds to the infinitesimal loss and infinitesimal gain at $u = 1$ ($z = 0$). For an (infinitesimal) loss in our system, we find

$$\begin{aligned} \psi(u) &= u^{i\sqrt{B}} \times {}_2F_1^*(-\sqrt{A} - i\sqrt{B}, \sqrt{A} - i\sqrt{B}, 1 - 2i\sqrt{B}, u - i0) \\ &+ ru^{-i\sqrt{B}} \times {}_2F_1^*(-\sqrt{A} + i\sqrt{B}, \sqrt{A}, 1 + 2i\sqrt{B}, u - i0), \end{aligned} \quad (14)$$

where the reflection coefficient is

$$\begin{aligned} r &= -\left[\frac{\Gamma(\sqrt{A} + i\sqrt{B}) \Gamma(1 + \sqrt{A} + i\sqrt{B})}{\Gamma(\sqrt{A} - i\sqrt{B}) \Gamma(1 + \sqrt{A} - i\sqrt{B})} \right]^* \\ &\times \frac{\Gamma(1 + 2i\sqrt{B})^* \exp(-2\pi\sqrt{B})}{\Gamma(1 + 2i\sqrt{B})}. \end{aligned} \quad (15)$$

In particular, when the in-plane wavenumber of the incident wave exceeds the maximum momentum supported by the dielectric at $z > d$, the field exponentially decays at $z > 0$, and for the reflection coefficient we find

$$|r|^2 = \exp(-4\pi\sqrt{B}) = \exp\left(-4\pi\sqrt{\varepsilon_1 + \frac{\varepsilon_1}{(-\varepsilon_-)} \frac{k^2 c^2 \omega d}{\omega^2}}\right). \quad (16)$$

Note that despite “total internal reflection” from the dielectric, the reflected wave contains only an (exponentially small) fraction of the incident energy—even an infinitesimal loss ($\Gamma \rightarrow +0$) leads to the absorption of nearly all incident energy. The origin of this behavior is the divergence of the electric field $E_z = \psi(z)/\varepsilon_z$, as according to Eq. (14) the wavefunction $\psi(0) \neq 0$ and $\varepsilon(0) = i0$. This situation is similar to the

field singularity at the positive-negative index metamaterial interface.²⁷

When the in-plane incident momentum $k < \sqrt{\varepsilon_1}\omega/c$ (so that $A < 0$), the dielectric medium to the right of the boundary layer can support the transmitted wave with the corresponding transmission coefficient:

$$t = \frac{2\sqrt{B}}{\sqrt{-A} + \sqrt{B}} \frac{\Gamma(2i\sqrt{-A})\Gamma(2i\sqrt{B})}{\Gamma(2i(\sqrt{-A} + \sqrt{B}))^2} \times \left[1 - \frac{\sinh^2(\pi(\sqrt{-A} - \sqrt{B}))}{\sinh^2(\pi(\sqrt{-A} + \sqrt{B}))} \right] \times \exp[-\pi(\sqrt{B} - \sqrt{-A})]. \quad (17)$$

When the transition layer thickness d is much larger than the free-space wavelength, $d \gg c/\omega$, the magnitude of the transmission coefficient is

$$|t|^2 \approx 4\sqrt{-\frac{B}{A}} \exp[-2\pi(\sqrt{B} - \sqrt{-A})] = 4\sqrt{\frac{1 + \frac{k^2c^2}{(-\varepsilon_-)\omega^2}}{1 - \frac{k^2c^2}{\varepsilon_1\omega^2}}} \exp\left[-2\pi\left(\sqrt{\varepsilon_1 + \frac{\varepsilon_1}{(-\varepsilon_-)}\frac{k^2c^2}{\omega^2}} - \sqrt{\varepsilon_1 - \frac{k^2c^2}{\omega^2}}\right)\frac{\omega d}{c}\right]. \quad (18)$$

In Fig. 3 we plot the intensity of the electric field $I_E(z) = E_x(z)^2 + E_z(z)^2$ (red/dark gray curve) and the intensity of the

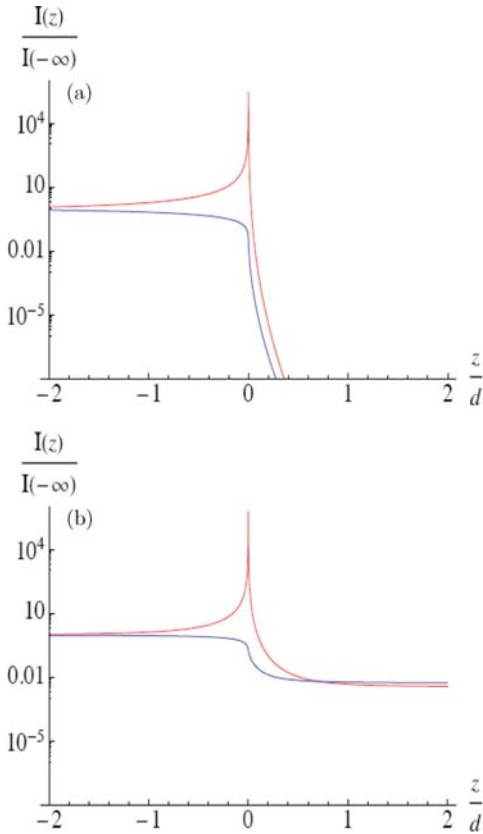


FIG. 3. (Color online) The electric (red/dark gray line) and magnetic (blue/medium gray line) field intensities for (a) $A = 30$, $B = 40$ and (b) $A = -30$, $B = 40$.

magnetic field $I_B(z) = B_y(z)^2$ (blue/medium gray curve) for both regimes: $k > \sqrt{\varepsilon_1}\omega/c$ in (a) and $k < \sqrt{\varepsilon_1}\omega/c$ in (b), in logarithmic scale. The $I_E(z) \sim 1/z^2$ divergence near $z = 0$ is clearly seen in both cases.

Now let us consider the case of a hyperbolic metamaterial interface, which is oriented perpendicular to the “spacelike” direction [Fig. 2(b)]. For the sake of simplicity, let us consider the case of constant $\varepsilon_2 = \varepsilon_z < 0$ and assume that finite $\varepsilon_1(x) = \varepsilon_x = \varepsilon_y$ changes sign from $\varepsilon_1 > 0$ to $\varepsilon_1 < 0$ as a function of x in some frequency range around $\omega = \omega_0$. Because of translational symmetry along the z direction, we may consider a plane wave solution in the z direction with a wave vector component k_z . Introducing $\psi = B$, as previously, we obtain

$$-\frac{\partial^2 \psi}{\partial x^2} + \frac{\varepsilon_2 k_z^2}{\varepsilon_1} \psi = \frac{\varepsilon_2 \omega_0^2}{c^2} \psi. \quad (19)$$

The same analysis as previously indicates that $E_x \sim -\frac{1}{\varepsilon_x} \frac{\partial \psi}{\partial z}$ diverges at the interface. Note that the choice of $\varepsilon_1 = \alpha x^2$ (where $\alpha > 0$) at $x = 0$ leads to Rindler-like optical space near the interface. The Rindler metric can be written as

$$ds^2 = -\frac{g^2 x^2}{c^2} dt^2 + dl^2, \quad (20)$$

where the horizon is located at $x = 0$.²⁸ The spatial line element of the corresponding Fermat metric as perceived by the Rindler observers is

$$dl^2 = \frac{dl^2}{-g_{00}} = \frac{c^4 dl^2}{g^2 x^2}. \quad (21)$$

Since the extraordinary photon wave vector $k \approx k_x \sim (-\varepsilon_2/\varepsilon_1)^{1/2} k_z$ diverges at the interface [see Eq. (19)], the “optical length” element experienced by the extraordinary photons also diverges:

$$dl_{\text{opt}}^2 = \frac{k^2 c^2 dl^2}{\omega_0^2} \sim \frac{dl^2}{x^2}, \quad (22)$$

where dl is the length element in the coordinate space. Comparison of Eqs. (21) and (22) demonstrates that a region of “optical space” near $x = 0$ does look like an electromagnetic black hole and $\alpha \sim g^2$ defines effective surface gravity at the horizon. However, we should emphasize that metamaterial losses lead to the appearance of the imaginary part in the effective potential $V = \frac{\varepsilon_2 k_z^2}{\varepsilon_1}$ in Eq. (19), so that no true horizon appears. An attempt to compensate losses with gain and achieve the “true horizon” would lead to effective Hawking radiation²⁸ from the interface. Due to divergent density of states in the hyperbolic band of the metamaterial,^{15,29} energy pumped into the metamaterial from the outside space would mostly go into the hyperbolic band around ω_0 . In the language of effective (2 + 1) Minkowski spacetime described by Eq. (3), new “particles” would be created at the boundary of this spacetime in the layer $\Delta x \sim 1/\alpha^{1/2}$. Due to the uncertainty principle, the momentum uncertainty of these particles is $\Delta p_x \sim \hbar \alpha^{1/2}$. At given ω_0 , this uncertainty translates into the same uncertainty $\Delta p_z \sim \hbar \alpha^{1/2} \sim T$ of the z component of the photon momentum, which plays the role of effective energy in the (2 + 1) Minkowski spacetime [see Fig. 1(c)]. Thus, we recover the well-known behavior of the Unruh–Hawking

effect:

$$\Delta p_z \sim T_H \sim \hbar \alpha^{1/2} \sim \hbar g. \quad (23)$$

Let us consider a possible experimental realization of these effects in the layered metamaterial structure presented in Fig. 1(b). Let us assume that the metallic layers are oriented perpendicular to z direction. The diagonal components of the permittivity tensor in this case have been calculated in Ref. 30 using Maxwell–Garnett approximation:

$$\varepsilon_1 = \alpha \varepsilon_m + (1 - \alpha) \varepsilon_d, \quad \varepsilon_2 = \frac{\varepsilon_m \varepsilon_d}{(1 - \alpha) \varepsilon_m + \alpha \varepsilon_d}, \quad (24)$$

where α is the fraction of metallic phase and $\varepsilon_m < 0$ and $\varepsilon_d > 0$ are the dielectric permittivities of metal and dielectric, respectively. We would like to arrange an “end of time” interface as a function of $\alpha(z)$. As described previously, we would like to keep ε_1 positive, while changing the sign of ε_2 . Simple analysis of Eq. (24) indicates that the “end of time” occurs around $\alpha_0 = \varepsilon_m / (\varepsilon_m - \varepsilon_d)$, while we need to keep $\varepsilon_d > -\varepsilon_m$ at the experimental frequency ω_0 . Thus, by gradually increasing α through the α_0 value we will observe the effect in question. This can be achieved by gradual increase of the metal layer thickness d_1 , while keeping the dielectric layer thickness d_2 constant, so that the necessary range of $\alpha = d_1 / (d_1 + d_2)$ is achieved. The Rindler horizon can be achieved in a similar manner.

While realization of the experimental geometry described previously would require complicated nanofabrication, a simpler experiment can be performed using Poly(methyl methacrylate) (PMMA)-based plasmonic hyperbolic metamaterials, described in detail in Ref. 22. Rigorous theoretical description of these metamaterials has been developed in Ref. 31. However, the following qualitative model may guide us in understanding similarity between the layered 3D hyperbolic metamaterials shown in Fig. 1(b) and plasmonic hyperbolic metamaterials (Fig. 4), which are based on PMMA

strips deposited onto gold film surface. Let us consider a surface plasmon (SP) wave which propagates over a flat metal-dielectric interface. If the metal film is thick, the SP wave vector is defined by the expression

$$k_p = \frac{\omega}{c} \left(\frac{\varepsilon_d \varepsilon_m}{\varepsilon_d + \varepsilon_m} \right)^{1/2}, \quad (25)$$

where $\varepsilon_m(\omega)$ and $\varepsilon_d(\omega)$ are the frequency-dependent dielectric constants of the metal and dielectric, respectively.³² Let us introduce an effective 2D dielectric constant ε_{2D} , which characterizes the way in which SPs perceive the dielectric material deposited onto the metal surface. Similar to the 3D case, we can introduce ε_{2D} so that $k_p = \varepsilon_{2D}^{1/2} \omega / c$, and, thus,

$$\varepsilon_{2D} = \left(\frac{\varepsilon_d \varepsilon_m}{\varepsilon_d + \varepsilon_m} \right). \quad (26)$$

Now it is easy to see that depending on the frequency, SPs perceive the dielectric material bounding the metal surface in drastically different ways. At low frequencies $\varepsilon_{2D} \approx \varepsilon_d$. Therefore, plasmons perceive a PMMA stripe as dielectric. On the other hand, at high enough frequencies around $\lambda_0 \sim 500$ nm, ε_{2D} changes sign and becomes negative since $\varepsilon_d(\omega) > -\varepsilon_m(\omega)$. As a result, around $\lambda_0 \sim 500$ nm plasmons perceive PMMA stripes on gold as if they are “metallic layers,” while gold/vacuum portions of the interface are perceived as “dielectric layers.” Thus, at these frequencies, plasmons perceive a PMMA stripe pattern from Fig. 4 as a layered hyperbolic metamaterial, shown in Fig. 1(b).

Rigorous description of plasmonic hyperbolic metamaterials in terms of Diakonov SPs³¹ produces similar results. In this description a PMMA grating on the gold film surface is treated as an anisotropic dielectric medium having the following perpendicular and parallel components (defined with respect

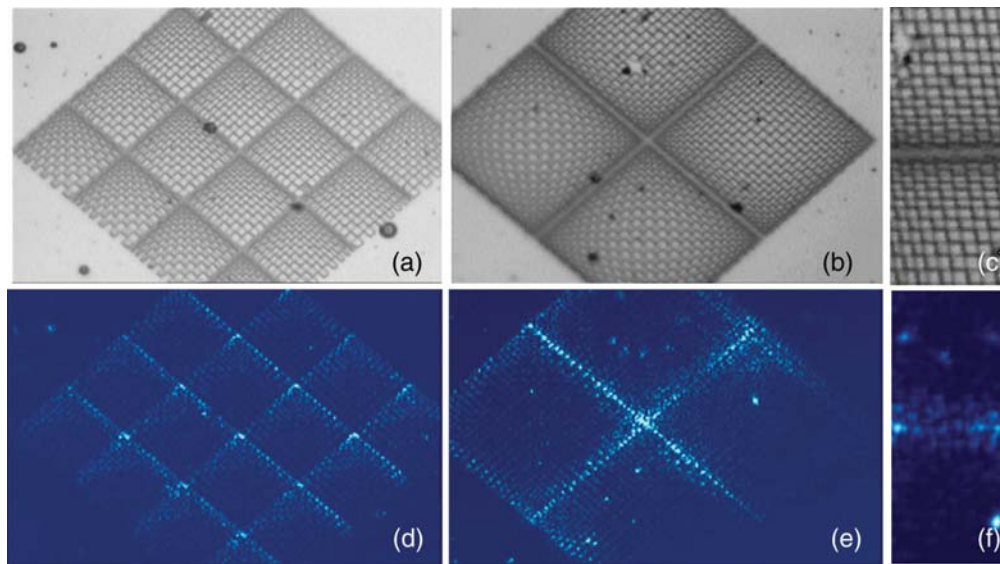


FIG. 4. (Color online) Experimental observation of the metric signature transition in a plasmonic hyperbolic metamaterial illuminated with 488 nm light. (a) and (b) Optical microscope images of the plasmonic metamaterial patterns illuminated with white light. (d) and (e) Same patterns illuminated with 488 nm laser light. (c) and (f) Digital zooms of the metric signature transition area.

to the optical axis) of the diagonal dielectric tensor:

$$\varepsilon_{\perp} = \alpha\varepsilon_d + (1 - \alpha), \quad \varepsilon_{\parallel} = \frac{\varepsilon_d}{(1 - \alpha)\varepsilon_d + \alpha}, \quad (27)$$

where ε_d is the permittivity of PMMA, and $\alpha = d_1/(d_1 + d_2)$ is defined by the widths d_1 and d_2 of the PMMA and vacuum stripes, respectively. In the frequency range below $\varepsilon_m(\omega) = -\varepsilon_{\perp}$ plasmon dispersion has normal elliptic character. On the other hand, in the frequency range between $\varepsilon_m(\omega) = -\varepsilon_{\perp}$ and $\varepsilon_m(\omega) = -(\varepsilon_{\perp}\varepsilon_{\parallel})^{1/2}$, the plasmon dispersion is hyperbolic. At $\alpha = 0.5$ this hyperbolic band is located between $\varepsilon_m(\omega) = -1.63$ and $\varepsilon_m(\omega) = -1.5$. According to material parameters of gold reported in Ref. 33, this frequency range is located around $\lambda = 490$ nm. Thus, the “end of time” conditions can be achieved in this frequency range via continuous variation of d_1 through the $\alpha = 0.5$ value in a plasmonic hyperbolic metamaterial.

Fabrication of such plasmonic hyperbolic metamaterials in two dimensions requires only very simple and common lithographic techniques. As described in the previous experimental scenario, the effective “metallic layer” width d_1 of PMMA stripes was varied, while the width of effective “dielectric layers” (the gold/vacuum portions of the interface) d_2 was kept constant. Because Eqs. (25) and (26) are approximations only, in the experiments presented in Fig. 4 we have used a PMMA bigrating geometry and varied its periodicity along both x and y directions within a broad range of parameters in order to achieve the presumed “end of time” conditions. Therefore, we followed the “combinatorial approach to metamaterials discovery,” as described in Ref. 34. The bigrating structures were defined using a Raith E-line electron beam lithography (EBL) system with ~ 70 nm spatial resolution. The written structures were subsequently developed using a 3:1 IPA/MIBK solution (Microchem) as developer. The fabricated structures were studied using an optical microscope under illumination with 488 nm Argon ion laser, as described in Ref. 22. It appears

that the optical images of field distribution over the sample surface do indicate considerable field enhancement near the presumed plasmonic metric signature transition events, as clearly seen in the digital zoom of the metric signature transition area shown in Fig. 4(f).

Compared to previous proposals of emulating a black hole event horizon using macroscopic electrodynamics (see, for example, Ref. 35 by Reznik), our technique appears to be much more practical. Experimental realization of Reznik’s proposal would require achieving infinite values of the dielectric permittivity ε inside the solid state black hole analog. While very large values of $\varepsilon \sim 1000$ may indeed be achieved in ferroelectrics in the limited frequency range, finite range of achievable ε leads to truncation of the attractive potential experienced by photons, so that no true horizon may appear. On the other hand, realization of our proposal relies on achieving ε near zero values [see Eq. (19)], which is much more practical. The main experimental difficulty in our case appears to be suppression of $\text{Im}(\varepsilon)$, which has been already demonstrated in metamaterials in the limited frequency range.³⁶

In conclusion, we have examined metamaterial optics at the boundaries of hyperbolic metamaterials. If the boundary is perpendicular to the spacelike direction in the metamaterial, an effective Rindler horizon may be observed, which produces Hawking radiation. On the other hand, if the boundary is perpendicular to the timelike direction the system undergoes a metric signature transition, with a nonintegrable electric field divergence at the transition point. Experimental observations of this transition using plasmonic metamaterials confirm the theoretical prediction.

This work was partially supported by ARO Multidisciplinary University Research Initiative Grants No. 50342-PH-MUR and No. W911NF-09-1-0539 and MRSEC program of the National Science Foundation.

*Corresponding author: smoly@eng.umd.edu

¹P. Horava, *Phys. Rev. D* **79**, 084008 (2009).

²J. B. Pendry, D. Schurig, and D. R. Smith, *Science* **312**, 1780 (2006).

³U. Leonhardt, *Science* **312**, 1777 (2006).

⁴U. Leonhardt and T. G. Philbin, *New J. Phys.* **8**, 247 (2006).

⁵I. I. Smolyaninov, *New J. Phys.* **5**, 147 (2003).

⁶I. I. Smolyaninov, *J. Opt.* **13**, 125101 (2011).

⁷D. A. Genov, S. Zhang, and X. Zhang, *Nature Physics* **5**, 687 (2009).

⁸E. E. Narimanov and A. V. Kildishev, *Appl. Phys. Lett.* **95**, 041106 (2009).

⁹Q. Cheng, T. J. Cui, W. X. Jiang, and B. G. Cai, *New J. Phys.* **12**, 063006 (2010).

¹⁰A. Greenleaf, Y. Kurylev, M. Lassas, and G. Uhlmann, *Phys. Rev. Lett.* **99**, 183901 (2007).

¹¹I. I. Smolyaninov, *J. Opt.* **13**, 024004 (2010).

¹²T. G. Mackay and A. Lakhtakia, *Phys. Lett. A* **374**, 2305 (2010).

¹³I. I. Smolyaninov and Y. J. Hung, *J. Opt. Soc. Am. B* **28**, 1591 (2011).

¹⁴L. Landau and E. Lifshitz, *The Classical Theory of Fields* (Elsevier, Oxford, 2000).

¹⁵I. I. Smolyaninov and E. E. Narimanov, *Phys. Rev. Lett.* **105**, 067402 (2010).

¹⁶P. A. M. Dirac, *Ann. Math.* **37**, 429 (1936).

¹⁷I. Bars and Y. C. Kuo, *Phys. Rev. Lett.* **99**, 041801 (2007).

¹⁸J. M. Romero and A. Zamora, *Phys. Rev. D* **70**, 105006 (2004).

¹⁹A. White, S. Weinfurter, and M. Visser, *Classical Quantum Gravity* **27**, 045007 (2010).

²⁰L. Landau and E. Lifshitz, *Electrodynamics of Continuous Media* (Elsevier, Oxford, 2004).

²¹Z. Jakob, L. V. Alekseyev, and E. Narimanov, *Opt. Express* **14**, 8247 (2006).

²²I. I. Smolyaninov, Y. J. Hung, and C. C. Davis, *Science* **315**, 1699 (2007).

²³Z. Liu, H. Lee, Y. Xiong, C. Sun, and X. Zhang, *Science* **315**, 1686 (2007).

²⁴G. Feinberg, *Phys. Rev.* **159**, 1089 (1967).

²⁵M. A. Noginov, Yu. A. Barnakov, G. Zhu, T. Tumkur, H. Li, and E. E. Narimanov, *Appl. Phys. Lett.* **94**, 151105 (2009).

- ²⁶G. N. Watson, *A Treatise on the Theory of Bessel Functions* (Cambridge University Press, Cambridge, 1944).
- ²⁷N. M. Litchinitser, A. I. Maimistov, I. R. Gabitov, R. Z. Sagdeev, and V. M. Shalaev, *Opt. Lett.* **33**, 2350 (2008).
- ²⁸C. Misner, K. S. Thorne, and J. A. Wheeler, *Gravitation* (W. H. Freeman, San Francisco, 1973).
- ²⁹Z. Jacob, I. I. Smolyaninov, and E. E. Narimanov, *Appl. Phys. Lett.* **100**, 181105 (2012).
- ³⁰R. Wangberg, J. Elser, E. E. Narimanov, and V. A. Podolskiy, *J. Opt. Soc. Am. B* **23**, 498 (2006).
- ³¹Z. Jacob and E. E. Narimanov, *Appl. Phys. Lett.* **93**, 221109 (2008).
- ³²A. V. Zayats, I. I. Smolyaninov, and A. Maradudin, *Phys. Rep.* **408**, 131 (2005).
- ³³D. R. Lide, Ed., *CRC Handbook of Chemistry and Physics* (CRC Press, Boca Raton, 2003).
- ³⁴E. Plum, K. Tanaka, W. T. Chen, V. A. Fedotov, D. P. Tsai, and N. I. Zheludev, *J. Opt.* **13**, 055102 (2011).
- ³⁵B. Reznik, *Phys. Rev. D* **62**, 044044 (2000).
- ³⁶S. Xiao, V. P. Drachev, A. V. Kildishev, X. Ni, U. K. Chettiar, H.-K. Yuan, and V. M. Shalaev, *Nature* **466**, 735 (2010).